

SRIA's Class L Mesh Elevated Slab Tests: Part 1B – Observations & Results

Scott Munter* and Mark Patrick**

* *Steel Reinforcement Institute of Australia, PO Box 418, Roseville, New South Wales, 2069, Australia (E-mail: scott.munter@sria.com.au)*

** *MP Engineers Pty Limited, 6 Doowi Court, Greensborough, Victoria, 3088, Australia (E-mail: mp-engs@bigpond.net.au)*

SLAB TEST OBSERVATIONS & RESULTS

Although considerable information was obtained from all of the tests about the serviceability behaviour of the slabs, the focus of this discussion is about ultimate load behaviour.

SSOW Test Series

Slab SSOW-TRIAL was a replica of slab SSOW-ST4, and was poured ahead of the rest of the SSOW slabs using mesh from a different batch, in preparation for trialling the new test rig and test procedure. The photograph in Fig. 7(a) shows the soffit of slab SSOW-ST7 at the positive hinge after the test. A Class L main mesh bar can be seen necked and fractured, while the adjacent N12 main bar remained intact. As expected, for all of the SSOW slabs the main mesh bars ultimately necked or fractured once the slabs had deflected sufficiently – see the last column of Table 2.

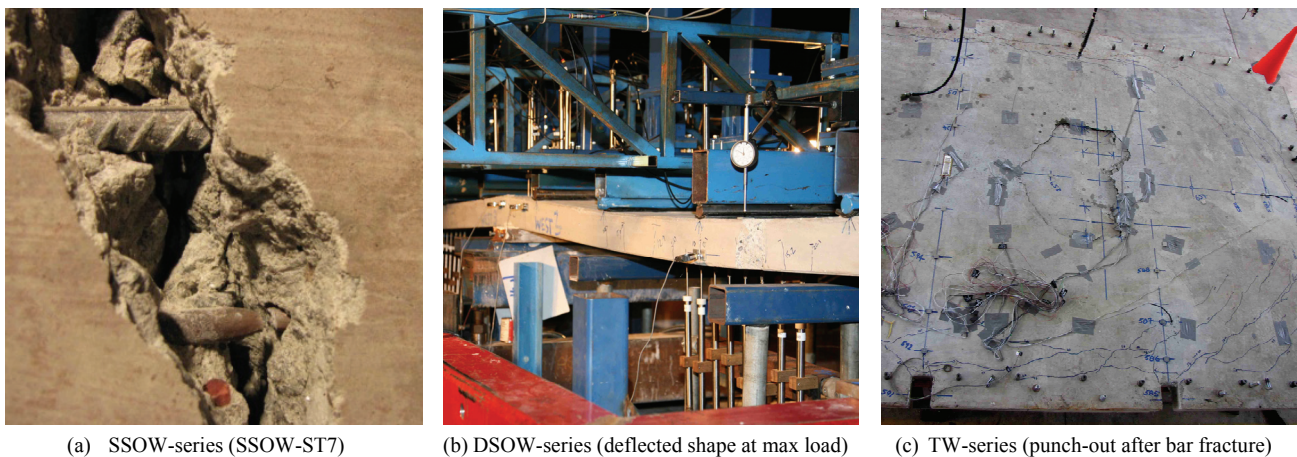


Figure 7. Test observations for SSOW, DSOW and TW test series.

In the test on slab SSOW-ST3, flexural failure occurred directly under the mid-span line load (see 2nd last column in Table 2). In all the other tests on unrestrained SSOW slabs (which therefore excludes slab SSOW-ST1 as it was restrained), the critical section occurred in the mid-span region between the inner pair of line loads, which was close to being a uniform-moment region while approaching and at ultimate load. In the test on slab SSOW-ST1, a positive hinge formed at mid-span, as expected due to compressive membrane action, and negative hinges formed at the inside edges of the ringbeam (see Fig. 3(c) of Part 1A of this paper).

The fourth last column in Table 2 shows the mid-span deflection of the SSOW slabs at maximum load. It can be seen that slab SSOW-ST3, with the single line load applied at mid-span, had by far the smallest mid-span deflection at ultimate load. Its load-deflection curve for Loading Stages III to V (see Part 1A) is shown in Fig. 8. Included on the same graph is the load-deflection curve for the nominally identical slab SSOW-ST2, loaded instead with four line loads to simulate design uniform loading conditions. This graph confirms that loading arrangement had a significant effect on the mid-span deflection reached at ultimate load. This was because, in the absence of a uniform-moment region (ST3), fewer less-developed flexural cracks would have developed along the span.

Table 2. Test results for SSOW, DSOW and TW test series.

Test Series	Test Specimen No.	Applied Load Configuration	Central Support Disp. (mm)	Total Applied Load per Span at 1 st Crack	Ultimate Total Applied Load per Span	Mid-span Defln at Max. Load (mm)	Mid-span Defln at 1 st Bar Fracture (mm)	Failure Cross-section Location/s	Failure Mode
SSOW	SSOW-ST1	4-line	-	42.0 kN/m	167.5 kN/m	33.6	48.0	Mid-span & ends	Mesh bar fracture
	SSOW-ST2	4-line	-	25.0 kN/m	46.6 kN/m	28.0	52.0	Mid-span region	Mesh bar fracture
	SSOW-ST3	1-line	-	15.8 kN/m	25.3 kN/m	18.8	>49.0	Mid-span	Mesh bar necking
	SSOW-ST4	4-line	-	24.0 kN/m	58.5 kN/m	40.0	60.0	Mid-span region	Mesh bar fracture
	SSOW-ST5	4-line	-	23.8 kN/m	93.1 kN/m	54.0	78.0	Mid-span region	Mesh bar fracture
	SSOW-ST6	4-line	-	22.0 kN/m	101.0 kN/m	55.0	77.0	Mid-span region	Mesh bar fracture
	SSOW-ST7	4-line	-	25.0 kN/m	84.0 kN/m	36.0	61.0	Mid-span region	Mesh bar fracture
	SSOW-ST8	4-line	-	23.0 kN/m	87.2 kN/m	45.0	66.0	Mid-span region	Mesh bar fracture
	SSOW-TRIAL	4-line	-	24.7 kN/m	56.8 kN/m	38.0	56.0	Mid-span region	Mesh bar fracture
DSOW	DSOW-ST1	4-line per span	-		168.0 kN/m	35.0	35.0	Mid-span & supports	Mesh bar fracture
	DSOW-ST2	4-line per span	5.0 up		163.0 kN/m	38.8	43.5	Mid-span & supports	Mesh bar fracture
	DSOW-ST3	4-line per span	-		91.0 kN/m	31.7	44.5	Inner & centre sup	Mesh bar fracture
	DSOW-ST4	4-line per span	5.0 up		90.0 kN/m	31.0	44.0	Inner & centre sup	Mesh bar fracture
TW	TW-ST1	Proof – water	-	-	15.5 kPa	2.6	-	-	Undamaged
		Ultimate – 4 pt	-	80 kN	445.0 kN	53.0	55.0	Yield-line pattern	Mesh bar fracture under patch loads

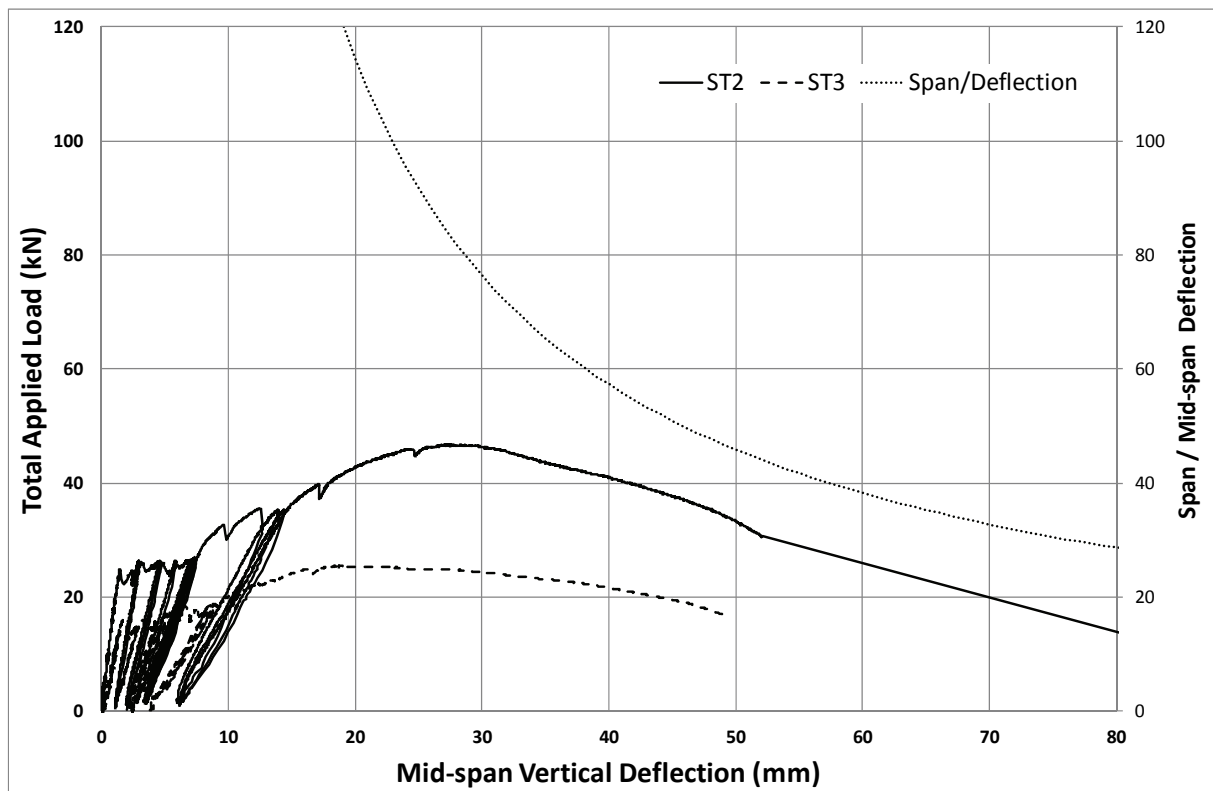


Figure 8. Load-deflection curves for slabs SSOW-ST2 and SSOW-ST3 (Loading Stages III to V).

Also plotted in Fig. 8 is the ratio of span ($L=2290$ mm for both slabs) to mid-span vertical deflection, shown on the right-hand vertical axis, against mid-span vertical deflection, shown on the horizontal axis. The resultant curve labelled “*Span/Deflection*” in Fig. 8 is arbitrarily truncated at a maximum value of this ratio equal to 120, i.e. 19.1 mm, which corresponds to a very large deflection, well in excess of normal design deflection limits for serviceability given in AS 3600. It can be seen that at ultimate load, the uniformly-loaded slab SSOW-ST2 attained a mid-span deflection of about span/80, or more precisely from Table 2, the ultimate total applied load was reached at 28.0 mm, or span/82. In contrast, on account of being non-uniformly loaded, slab SSOW-ST3 reached its ultimate strength at a smaller mid-span deflection of span/122, which nevertheless is still large. It follows that in practice, both slabs SSOW-ST2 and SSOW-ST3 would exceed normal serviceability deflection limits well before either could fail by strength.

It is clear by comparing the ultimate total applied loads for slabs SSOW-ST4 (SL102 only), SSOW-ST5 (SL102 + N12@500 bottom) and SSOW-ST6 (SL102 + N12@333 top) given in the sixth column of Table 2, that adding N12 bars significantly and consistently increased load-carrying capacity. (Note: in accordance with the effective depths provided in Table 1 of Part 1A, the Class N main bars were tied underneath the mesh in SSOW-ST5, and on top of the mesh in SSOW-ST6, with minimum concrete cover measured to the mesh bottom main bars.) Therefore, the Class L mesh bars and individual Class N bars acted together as main tensile reinforcement to increase the flexural strength of the under-reinforced critical cross-sections. Furthermore, comparing their mid-span deflections at ultimate load, it is apparent that adding the more ductile N12 bars also increased the slab deformation at ultimate load, i.e. compare 40, 54 and 55 mm for slabs SSOW-ST4, ST5 and ST6, respectively. These increases in load-carrying capacity and deflection at maximum load are particularly evident when comparing the load-deflection curves for the three slabs, shown in Fig. 9. Similar to Fig. 8, the curve labelled “*Span/Deflection*” in Fig. 9 shows that all three slabs attained large mid-span deflections at ultimate load in excess of span/60, with slabs SSOW-ST5 and SSOW-ST6 reaching close to span/40.

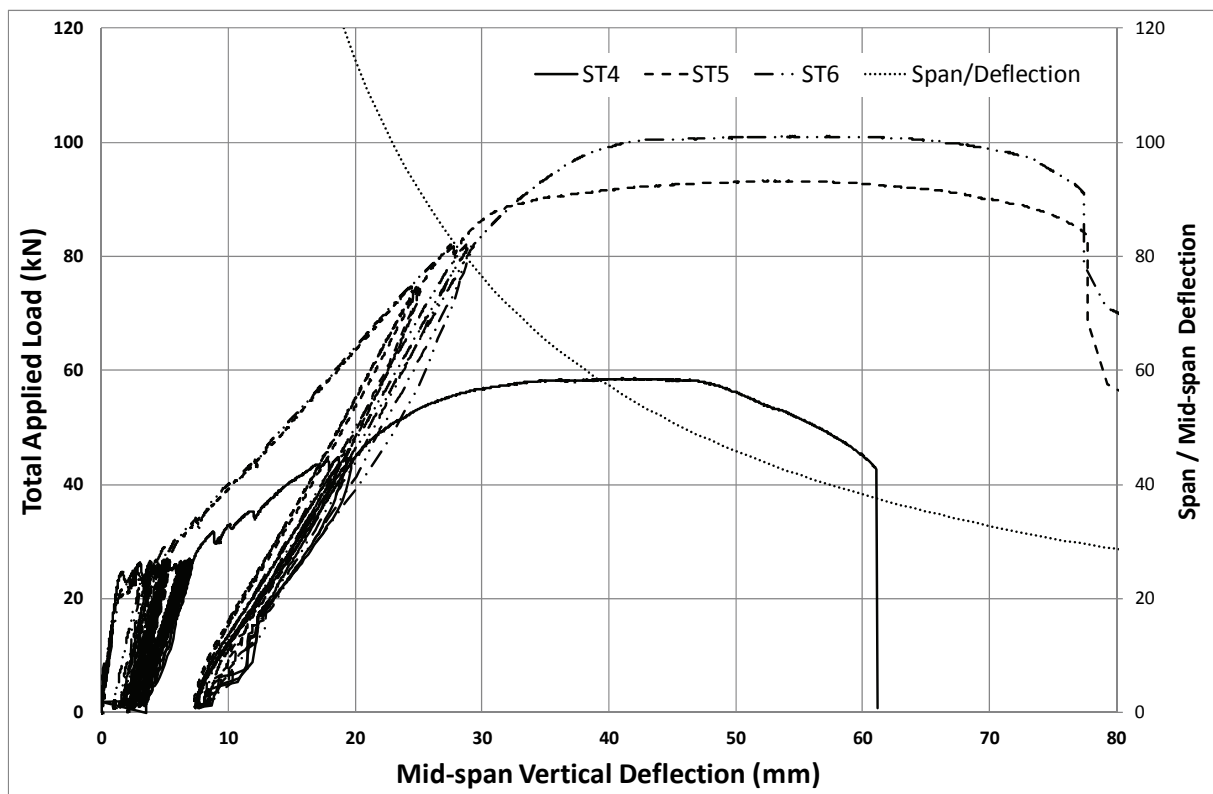


Figure 9. Load-deflection curves for slabs SSOW-ST4, SSOW-ST5 and SSOW-ST6 (Loading Stages III to V).

Comparing the load-deflection curves shown in Fig. 10 for slabs SSOW-ST2 (SL92 only), SSOW-ST7 (SL92 + N12@500 bottom) and SSOW-ST8 (SL92 + N12@333 top), similar conclusions apply for these slabs. The N12 bars greatly increased the load-carrying capacity of slabs SSOW-ST7 and SSOW-ST8 compared with the slab with the mesh only (SSOW-ST2), and their mid-span deflections at ultimate load of span/64 and span/51, respectively, were also significantly larger than the nevertheless large value of span/82 for slab SSOW-ST2.

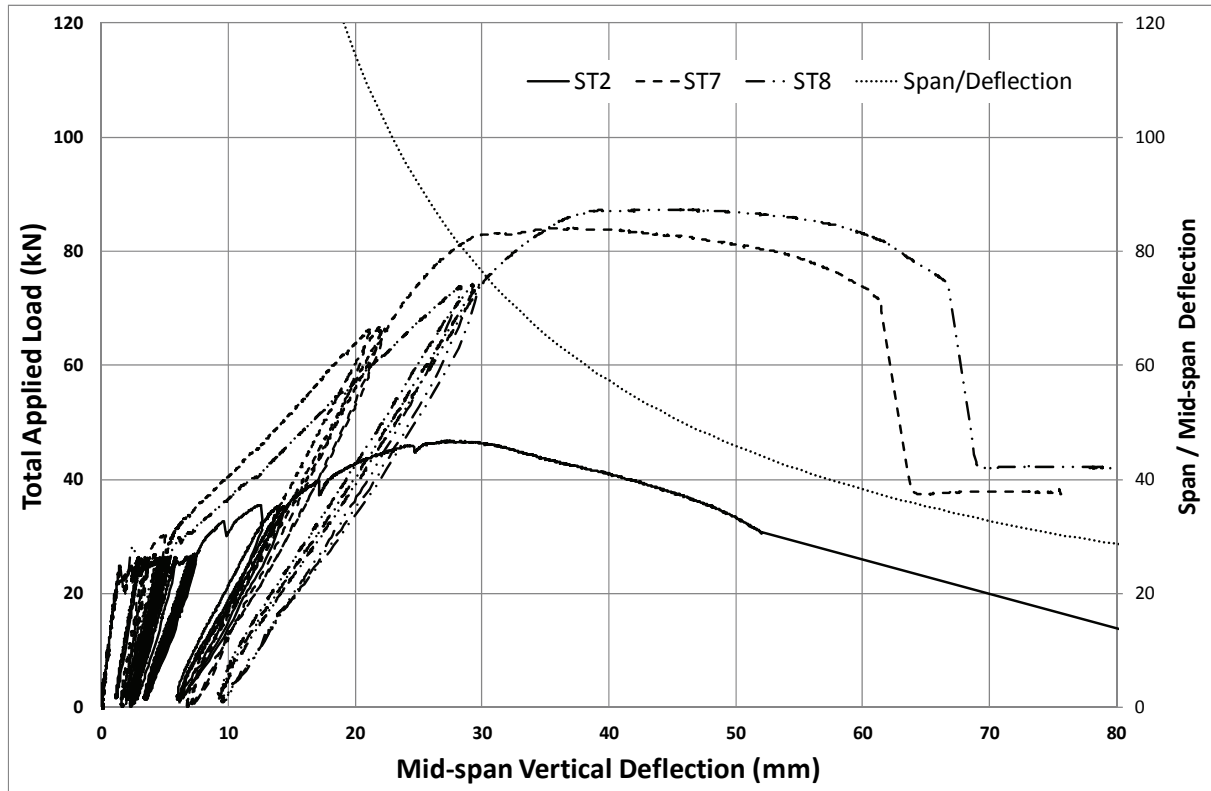
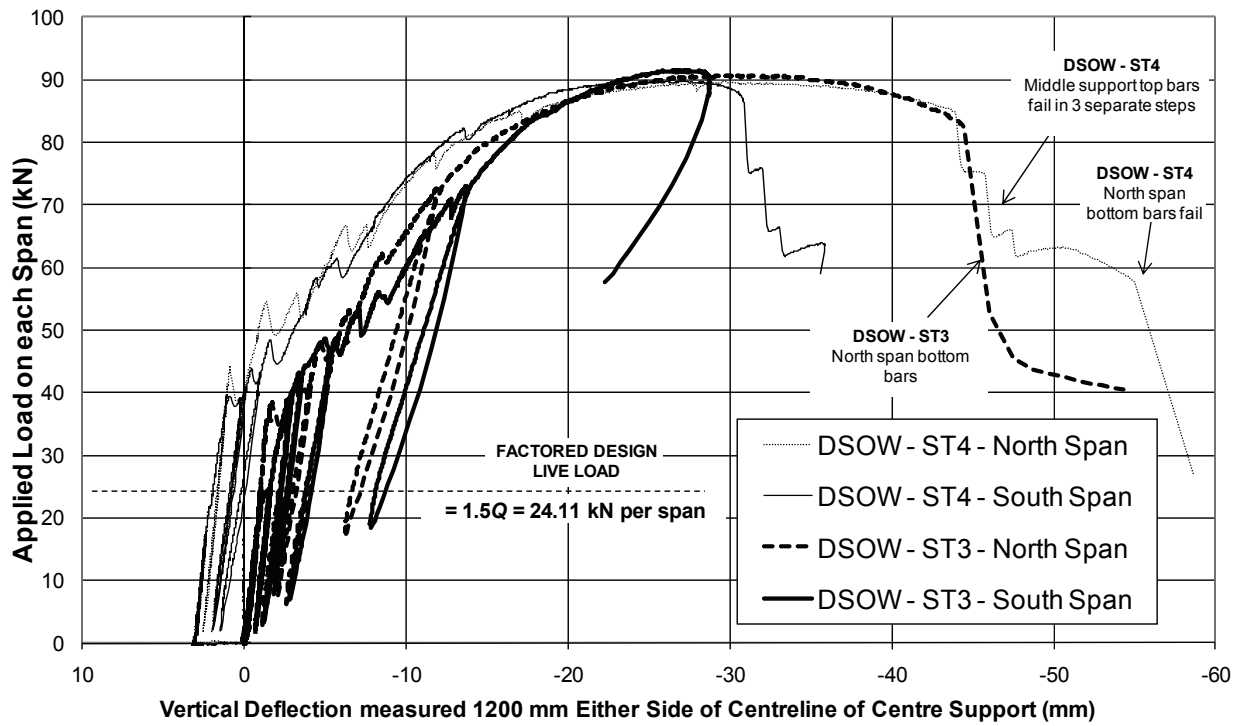


Figure 10. Load-deflection curves for slabs SSOW-ST2, SSOW-ST7 and SSOW-ST8 (Loading Stages III to V).

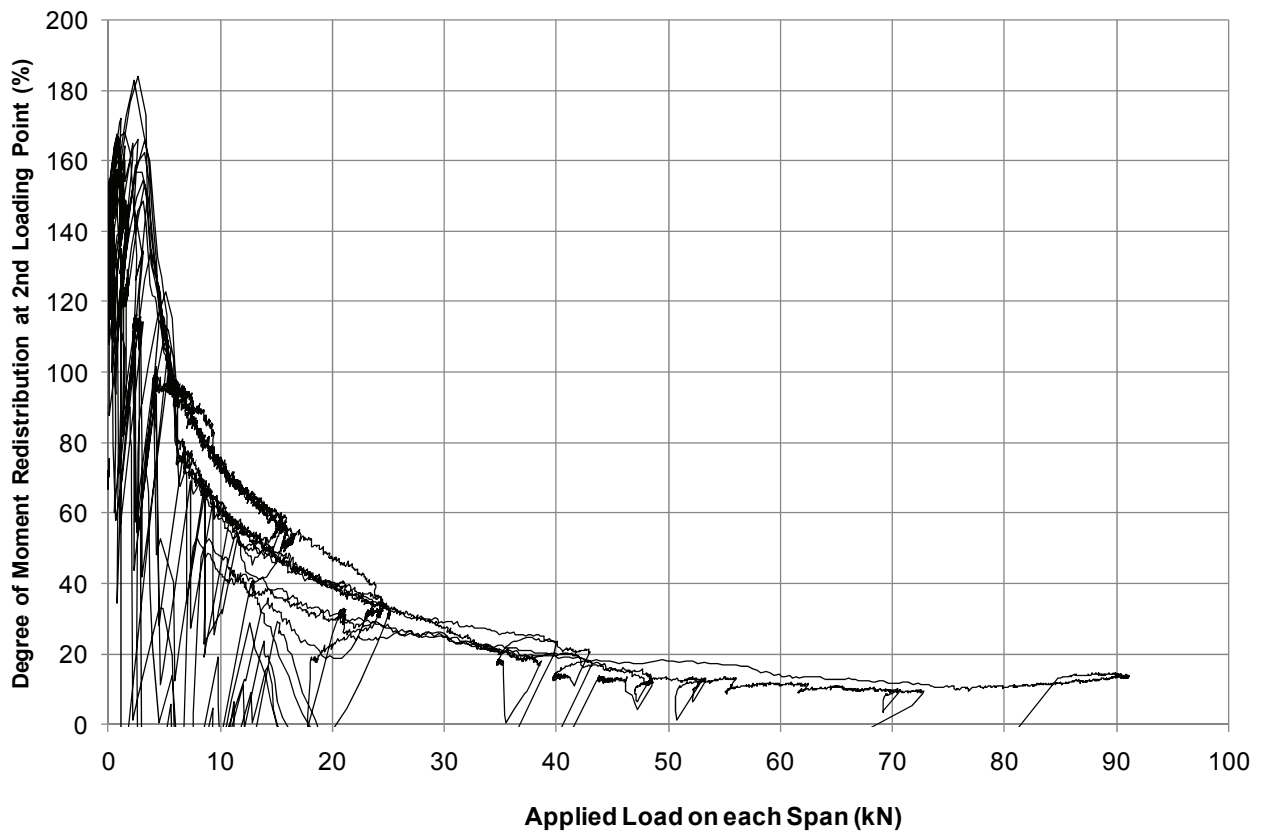
Finally, as was intended during design, all of the values of ultimate applied load (6th column in Table 2) well exceed the applied load recorded to cause the first flexural crack (5th column).

DSOW Test Series

The results in the 6th column of Table 2 for the two pairs of restrained or unrestrained DSOW slab tests show that the relative support settlement of 5 mm imposed before loading the slabs to failure had an insignificant effect on the maximum (ultimate) load reached in these tests. (However, a detailed study of the results showed that it did affect the sequence in which the negative and positive plastic hinges formed.) The restrained slabs DSOW-ST1 and ST2 reached their maximum load at slightly greater deflections than unrestrained slabs DSOW-ST3 and ST4 (see Fig. 7(b), and curves for the last stage of loading in Fig. 11(a)). They were similar to that of restrained slab SSOW-ST1. The degree of moment redistribution that occurred at the location of the positive plastic hinge formed under the line load 2nd in from the pinned end of slab DSOW-ST3 is plotted in Fig. 11(b) as a function of the applied load per span, which shows that a very large amount of moment redistribution occurred under serviceability conditions, but that this diminished as plastic hinges formed and the bending moment distribution was eventually controlled to a significant degree by the layout and mechanical and geometric properties of the main steel reinforcement comprising Class L mesh in the top and bottom faces. That is to say, detailed analysis of the test results for unrestrained slabs DSOW-ST3 and ST4 showed that in both tests, very close to a complete plastic hinge mechanism formed, with the maximum moment capacities of critical cross-sections in positive or negative bending almost being reached coincidentally.



(a) Load-deflection curves (DSOW-ST3 & DSOW-ST4)



(b) Moment redistribution at positive hinge (DSOW-ST3)

Figure 11. Results for DSOW-ST3 and DSOW-ST4 slabs.

TW Test Series

The two-way slab was uncracked during the proof load test to its design ultimate load. As Fig. 7(c) shows, it eventually failed under a pair of patch loads when the main bottom mesh bars broke, which gives the wrong impression of a punch-out failure. At the instant the bars broke, the load was close to its maximum and failure appeared sudden, but as seen from Table 2 and Fig. 12, deflection was very large at around span/40, with the span assumed to equal 2250 mm, i.e. in accordance with Clause 1.7 of AS 3600, short clear span of 2140 mm plus nominal overall slab depth of 110 mm.

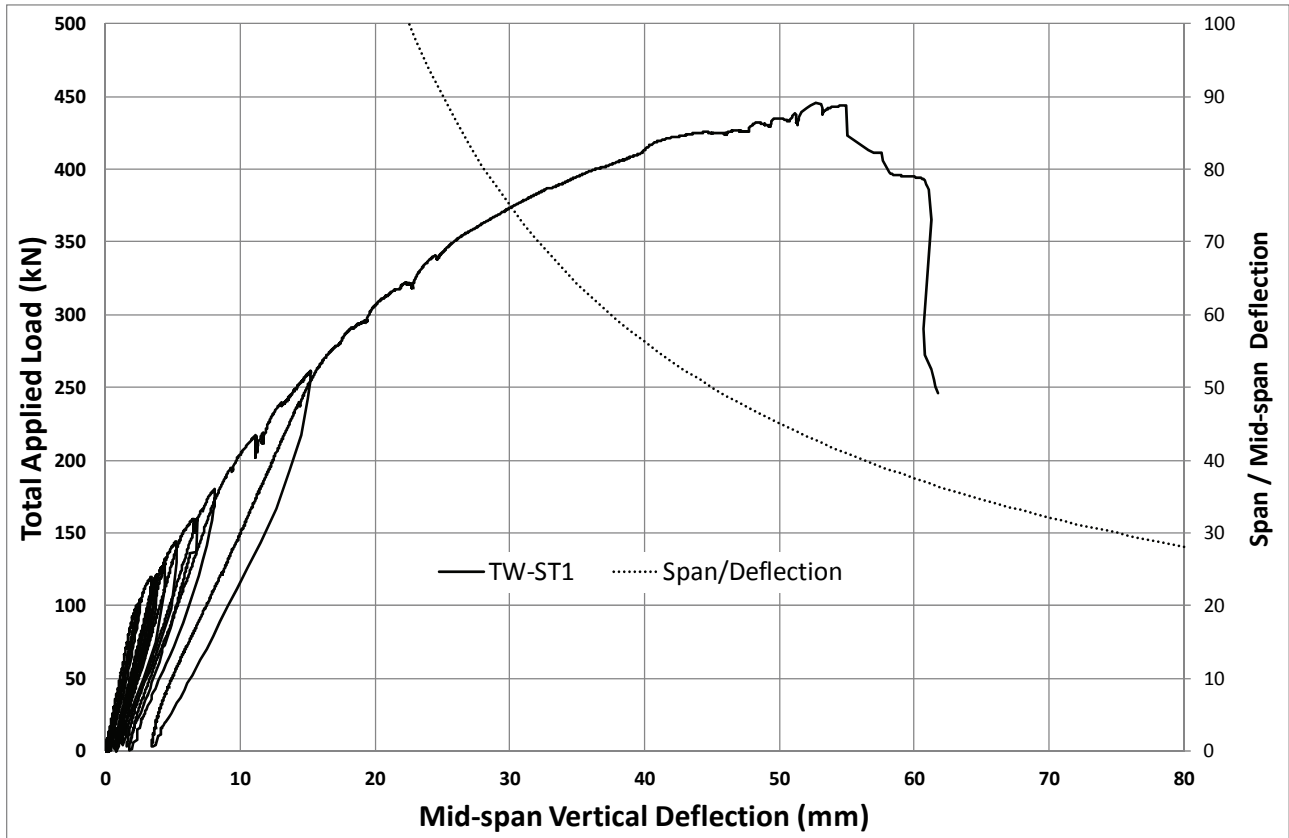


Figure 12. Load-deflection curves for slab TW-ST1 (Final Loading Stage).

MEASURED SLAB GEOMETRIES AND MATERIAL PROPERTIES

Slab Geometries

The average overall depth, D , of the SSOW, DSOW and TW slabs measured was 112 mm for each series, very close to the nominal value of 110 mm. Average measured concrete cover, c , to the closest bottom bars was 23, 20 and 19 mm for the SSOW, DSOW and TW-series slabs, respectively, while for the top steel the corresponding values were 20, 25 and 19 mm.

Material Properties

Concrete. The SSOW-TRIAL slab was poured before the other SSOW slabs, which were all poured together. The four DSOW slabs were poured separately, but also all together. The TW-series slab was poured separately again. The average density of the concrete was 2350, 2360 and 2365 kg/m³ for the SSOW (SSOW-TRIAL excepted), DSOW and TW-series slabs, respectively. The specified strength grade of the concrete was 32 MPa, and the mix design was constant being from the same supplier. The mean cylinder compressive strength of the concrete determined over the period of testing was 35.5 MPa (88-102 days old), 42.0 MPa (112-132 days old) and 33.0 MPa (44-49 days old) for SSOW (SSOW-TRIAL excepted), DSOW and TW-series slabs, respectively.

Reinforcing steels. Based on the test data most relevant to each test slab (SRIA, 2012 & Curtin University and SRIA, 2011), the average tensile properties of the main bars for the SSOW, DSOW and TW-series tests are given in Table 3. Nominal cross-sectional areas for SL102 mesh, SL92 mesh and N12 bars of 354 mm²/m, 290 mm²/m and 113 mm², respectively, were used. The values of the tensile parameters of all the SL92 and SL102 reinforcing meshes and N12 bar used in the SSOW, DSOW and TW-series slabs satisfied the conformance criteria of Paragraph B4 of AS/NZS 4671. Bar surface geometry met the requirements of Table 6.1 in AS/NZS 4671.

Table 3. Mean tensile properties of main steel bars for SSOW, DSOW and TW test series.

Test Series	Test Specimen No.	Bottom Steel	Proof/Yield Stress (MPa)	Tensile Stress (MPa)	Uniform Strain (%)	Top Steel	Proof/Yield Stress (MPa)	Tensile Stress (MPa)	Uniform Strain (%)
SSOW	SSOW-ST1	SL102	568.3	602.0	2.87	SL92	567.5	596.0	2.40
	SSOW-ST2	SL92	571.1	597.4	2.30	-	-	-	-
	SSOW-ST3	SL92	567.5	596.0	2.40	-	-	-	-
	SSOW-ST4	SL102	568.3	602.0	2.87	-	-	-	-
	SSOW-ST5	SL102/N12	568.3 / 540.8	602.0 / 636.2	2.87 / 11.66	-	-	-	-
	SSOW-ST6	SL102/N12	568.3 / 540.8	602.0 / 636.2	2.87 / 11.66	-	-	-	-
	SSOW-ST7	SL92/N12	567.5 / 540.8	596.0 / 636.2	2.40 / 11.66	-	-	-	-
	SSOW-ST8	SL92/N12	567.5 / 540.8	596.0 / 636.2	2.40 / 11.66	-	-	-	-
	SSOW-TRIAL	SL102	582.0	621.7	4.44	-	-	-	-
DSOW	DSOW-ST1	SL92	571.4	612.2	3.34	SL102	582.8	614.3	3.41
	DSOW-ST2	SL92	586.0	624.1	3.66	SL102	587.7	618.7	3.41
	DSOW-ST3	SL92	595.4	634.6	3.66	SL102	595.8	627.5	3.41
	DSOW-ST4	SL92	595.2	636.8	3.66	SL102	566.8	590.2	2.85
TW	TW-ST1 (Short)	SL102	567.0	602.7	2.65	SL92	580.7	611.0	2.17
	TW-ST1 (Long)	SL102	585.0	608.0	3.40	SL92	577.7	618.7	3.70

CONCLUSIONS

Details of a major experimental investigation into the behaviour of elevated slabs incorporating Class L mesh undertaken at Curtin University for the SRIA have been briefly described. The test objectives and design of the test specimens to AS 3600–2009 were explained, with strength and structural safety critical aspects of the investigation. The main test results relating to the ultimate strength limit state, and all the necessary information about the test set-ups and the geometric and material properties of the test slabs have been detailed in this first part of the paper, in preparation for the second part which for the first time in Australia presents the test results in relation to their minimum design requirements.

ACKNOWLEDGEMENT

The authors wish to acknowledge the support of their respective organisations to prepare this paper.

REFERENCES

- Blakey, F.A. (1963). *Australian Experiments with Flat Plates*. Journal of the American Concrete Institute, April.
- Chandler, I. and Lloyd, N. (2012). *Test Report – SRIA Class L Mesh Slab Tests: Vol. 1 (Report); Vol. 2 (Plates); and Vol. 3 (Figures)*. School of Civil and Mechanical Engng, Dept. of Civil Engng, Curtin University.
- Curtin University and SRIA (2011). *SRIA Class L Mesh Slab Tests conducted for SRIA (Supplement): Strength Design of SSOW, DSOW & TW Slab Test Specimens in accordance with AS 3600–2009; and Comparison with Test Results*.
- Munter, S., Patrick, M. and Rangan, B.V. (2010). *Review of Australian Support-Settlement Tests on Continuous, One-Way Reinforced-Concrete Slabs incorporating Low-Ductility Reinforcement*.

Proc. Australasian Structural Engineering Conference.

Patrick, M. and Keith, J. (2008). *New Developments in the Testing, Design and Construction of Concrete Structures incorporating Class L Reinforcing Mesh*. Steel Reinforcement Institute of Australia.

Sakka, Z.I. and Gilbert, R.I. (2008). *Strength and Ductility of Corner Supported Two-Way Concrete Slabs containing Welded Wire Fabric*. UNICIV Report No. R-453, University of New South Wales, October.

Sakka, Z.I. and Gilbert, R.I. (2009). *Ductility of Edge-Supported Two-Way Concrete Slabs containing Class L Reinforcement*. UNICIV Report No. R-454, University of New South Wales, May.

Standards Australia (SA) (2001). *Steel Reinforcing Materials*. AS/NZS 4671–2001.

Standards Australia (SA) (2002). *Structural Design Actions, Part 0: General Principles*. AS/NZS 1170.0–2002.

Standards Australia (SA) (2009). *Concrete Structures*. AS 3600–2009.

Steel Reinforcement Institute of Australia (SRIA) (2008). *Design to AS 3600–2001 of Suspended Concrete Floors Reinforced with Class L Mesh*. Technical Note No. TN6, March.

Steel Reinforcement Institute of Australia (SRIA) (2012). *SRIA Class L Mesh Slab Tests: Analysis of Steel Reinforcement Property Results*.